Structure of Rapidly Quenched Li_2O-SiO_2 Glasses†

Nobuya IWAMOTO*, Norimasa UMESAKI, Masahiro TATSUMISAGO*** and Tsutomu MINAMI*****

Abstract

Raman spectra of four glasses in the Li_2O-SiO_2 system ($41.3 \leqq Li_2O \leqq 61.3$ mole%) prepared by rapid quenching were measured. The proportions of SiO_4 units with 1, 2, 3 and 4 non-bridging oxygens per silicon (NBO/Si) and the fractions of bridging oxygens, non-bridgingoxygen and free or fully-active oxygen were estimated for these glasses from the quantitative analysis of the obtained Raman spectra. X-ray structural analysis of the Li_2O-SiO_2 glasses were found to elongate the average atomic distance of Si-O pair with the increase of the Li_2O content due to the weaking of the Si-O bond.

KEY WORDS : (Raman spectroscopy) (X-ray structural analysis) (Rapid quenching) (Li_2O-SiO_2 glasses) (Lithium silicate glasses)

1. Introduction

Rapid quenching is one of the useful technique to develop new glassy materials and to extend the composition range of glass formation. In the system Li_2O-SiO_2, Tatsumisago[1,2] indicated that the rapid quenching extended the limit of the glass formation from 40 mole% Li_2O for usual melt-cooling method up to 66.7 mole% Li_2O, which corresponds to the composition of lithium orthosilicate $2Li_2O \cdot SiO_2$, and the ratio T_g/T_l (T_g: glass transition temperature; T_l: liquidus temperature) of the Li_2O-SiO_2 glasses deviated from the so-called "Two-Third Rule" ($T_g/T_l = 2/3$) with increasing Li_2O content. They[3] also found from the density measurement that the rapidly quenched Li_2O-SiO_2 glasses have an "Open Structure". Our recent MD (Molecular Dynamics) results[4,5] of $2Li_2O \cdot SiO_2$ melt and glass have revealed that this glass consists of some discrete SiO_4 units with 2, 3 and 4 NBO/Si's (NBO/Si: Non-Bridging Oxygen per Si) because of the freezing of the corresponding melt by the rapid quenching. Therefore, these new dimensional silicate network structure cannot be formed at such a composition.

Raman spectroscopy is a powerful method for the identification of distinct SiO_4 units in silicate crystals and glasses. The stretching vibration modes of Si-O bonds in silicate crystals and glasses can easily be observed in the frequency region from 800 to 1200cm^{-1} by Raman spectroscopy. Many earlier investigations on slicate glasses were reported[6-11]. Mysen and his coworkers[7,8] pointed out the coexistence of anionic SiO_4 species such as SiO_4^{4-} monomer (NBO/Si=4), $Si_2O_7^{6-}$ dimer (NBO/Si=3), SiO_3^{2-} chain (NBO/Si = 2), $Si_2O_5^{2-}$ sheet (NBO/Si = 1) and SiO_2^0 three-dimensional network unit (NBO/Si=0) in alkali and alkaline earth silicate glasses from their Raman results. Tsunawaki et al.[9,10] determined the fractions of bridging oxygen "$-O-$" or "O^0" (i. e., coordinated to two Si^{4+}), non-bridging oxygen "O^-"(i. e., coordinated to one Si^{4+}) and free or fully active "O^{2-} (i. e., not coordinated to Si^{4+}) in glasses PbO-SiO_2, CaO-SiO_2 and CaO-SiO_2-CaF from Raman intensities of Si-O stretching bands. Furukawa et al.[11] remeasured glasses in the system Na_2O-SiO_2 in details.

It is the purpose of this study to reveal the structures of the rapidly quenched Li_2O-SiO_2 glasses by Raman spectroscopy. Based on the Raman result, we discussed the abundance of the SiO_4 units existing in these glasses. Furthermore, in order to obtain the information of the Li_2O-SiO_2 glass structures such as the atomic distance and the coordination number, X-ray diffraction study was carried out.

† Received on October 31, 1988

* Professor Welding Research Institute, Osaka University, 11-1, Mihogaoka

** Research Instructor Welding Research Institute, Osaka University, 11-1, Mihogaoka

*** Department of Applied Chemistry, University of Osaka Prefecture, Mozu-Umemachi, Sakai, Osaka 591

Transactions of JWRI is published by Welding Research Institute of Osaka University, Ibaraki, Osaka 567, Japan

2. Experimental

The Li_2O-SiO_2 glasses were prepared by the twin-roller apparatus with a thermal-image furnace, which was reported previously[1]. **Table 1** provides a list of nominal compositions of the starting materials and analyzed compositions of the prepared glasses.

Raman spectra were measured with a JASCO model R-800 double-grating spectrophotometer. The excitation source was the 514.5 Å (19435.6cm^{-1}) line of NEC GLG − 3300 Ar-ion laser power level from 300 to 400 mW. Each Raman spectrum obtained was deconvoluted into several Gaussian peaks using a nonlinear least square procedure. The calculated by the following equation.

$$I_R = \sum_{i=1} I_i \exp\{-1n2[2(\omega-\omega_i)/\Delta\omega_i]^2\}, \quad (1)$$

where I_i, ω_i and $\Delta\omega_i$ are the intensity, position and half-width of the peak i, respectively. The area of this Gaussian peak i to total area, A_i, that is, the relative intensity, is expressed by

$$A_i = [1/2\sqrt{(\pi/1n2)I_i\Delta\omega_i}\,]/I_R. \quad (2)$$

Deconvolution of the spectrta was carried out for the digitized scattering data by microcomputer[12].

X-ray diffraction measurement was carried out by Rigaku Denki X-ray diffractometer with a rotating anode generator, RAD-rA, with Mok $\bar{\alpha}$ ($\lambda = 0.7107$ Å) radiation under 50 kW-120 mA. The X-ray scattering intensities were measured from $\theta = 3°$ to $70°$ at $0.25°$ intervals using the step-scanning technique with a fixed time of 200sec. After the correction of background, polarization and Compton scattering, the coherent X-ray intensities, $I_{en}^{ceh}(S)$, were scaled by means of the high-angle region method and the Krong-Moe, Norman's method to the theoretical intensities due to the independent atoms contained. The radial distribution function, D(r), were obtained from the reduced intensity, S·i(S).

$$S\cdot i(S) = S[I(S)/\sum_{i=1}^{m} f_i(S)^2 - 1], \quad (3)$$

$$D(r) = 4\pi r^2\rho_0\sum_{i=1}^{m}\bar{K}_i + \sum_{i=1}^{m}(\bar{K}_i)^2(2r/\rho_0)\int_0^{Smax} S\cdot i(S)\sin(Sr)ds, \quad (4)$$

where m is the number of atoms contained in the stoichiometric units, ρ_0 the mean atomic density, $f_i(S)$ the atomic scattering factor of atom i corrected for anomalous dispersion, $\bar{K}_i$ the effective electron number of atom i and S_{max} the maximum value of S ($= 4\pi\sin\theta/\lambda$). The function, D(r)/r, calculated from the obtained X-ray intensities were deconvoluted into some Gaussian peaks based on the nonlinear least square procedure for the determination of the distances ($r_{i-j} \pm 0.01$Å) and coordination number ($N_{i/j} \pm 0.1$ atoms) of the nearest-neighbor atomic pairs i-j in these glasses. We used the density values[3] of these glasses determined by the heavy solution method, using a mixture of bromoform and carbon tetrachloride as a heavy solution. The detailed procedure for the measurement and the calculation method of the X-ray data were reported elsewhere[13].

3. Results and discussion

Figure 1 shows the Raman spectra of the Li_2O-SiO_2 glasses prepared by rapid quenching. The bands appearing these Raman spectra can be grouped conveniently into

Table 1 Mixed and analyzed compositions of the rapidly quenched Li_2O-SiO_2 glasses.

Glass sample	Li_2O (mol%)		SiO_2 (mol%)		NBO/Si
	mixed	analyzed	mixed	analyzed	number+
$2Li_2O\cdot SiO_2$	67.0	63.0	33.0	37.0	3.405
$3Li_2O\cdot SiO_2$	60.0	59.6	40.0	40.4	2.951
$Li_2O\cdot SiO_2$	50.0	50.4	50.0	49.6	2.032
$2Li_2O\cdot 3SiO_2$	40.0	41.3	60.0	58.7	1.407

+ NBO/Si: Non-Bridging Oxygen per Si

two frequency regions, 500 ~ 750cm^{-1} and 800 ~ 1200cm^{-1}. As shown in this figure, with the increases of the Li_2O content, the bands at 500~750cm^{-1}, which are assigned to the bridging Si-O-Si vibration[15] and labeled as B in Fig. 1, greatly reduce their intensities and shift toward higher frequency region. The continuous intensity drop and shift in the position of the B band with increasing the Li_2O must be related to the depolymerization between SiO_4 units. The 800~1200cm^{-1} frequency part of the measured Raman spectra are attributed to the non-bridging Si-O stretching mode of four SiO_4 units with 1, 2, 3 and 4 NBO/Si's, that is, $Si_2O_5^{2-}$ sheet, SiO_3^{2-} chain, $Si_2O_7^{6-}$ dimer and SiO_4^{4-} monomer [7-11]. As summarized in **Table 2**, these four Raman modes caused by the SiO_4 units with1, 2, 3 and 4 NBO/Si's appear on 1030~1100cm^{-1}, *950* ~ 970cm^{-1}, 900 ~ 930cm^{-1} and 850 ~ 890cm^{-1}, respectively. In glasses containing relatively small amount of Li_2O, the main peaks are the bands due to the $Si_2O_5^{2-}$ sheet and SiO_3^{2-} chain. On the other hand, in glasses containing large amount of Li_2O, the bands due to $Si_2O_7^{6-}$ dimer and SiO_4^{4-} monomer are mainly observed. This Raman result indicates that the SiO_4 units with higher NBO/Si ratio increase with the increase of the Li_2O content because of the depolymeriza-

Table 2 Raman frequencies due to the Si-O stretching mode due to SiO_4 units with 0, 1, 2, 3 and 4 NBO/Si's in alkali and alkaline earth silicate glasses[6-11].

SiO_4 unit	Bonding state of bound oxygen	NBO/Si number	Frequency (cm^{-1})
SiO_2^0 three-dimensional network	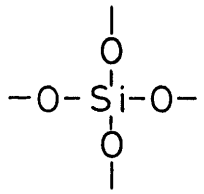	0	1060 - 1065 1190 - 1200
$Si_2O_5^{2-}$ sheet	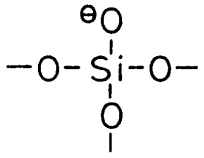	1	1030 - 1100
SiO_3^{2-} chain	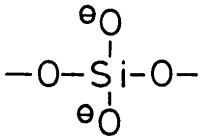	2	950 - 970
$Si_2O_7^{6-}$ dimer	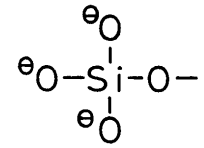	3	900 - 930
SiO_4^{4-} monomer	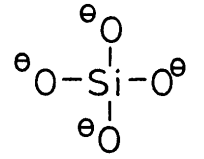	4	850 - 890

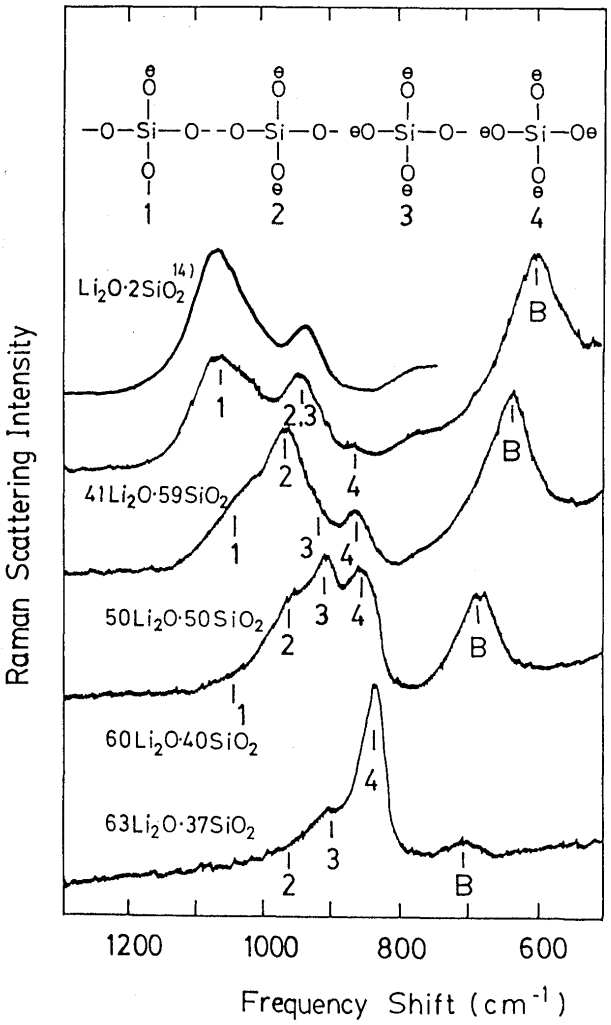

Fig. 1 Raman spectra of the rapidly quenched Li_2O-SiO_2 glasses. Included in this figure for comparison is the Raman spectrum of Li_2O-SiO_2 glass[14].

tion between SiO_4 units.

Figure 2 shows the Raman spectrum of $63Li_2O \cdot 37SiO_2$ glass deconvoluted into three Gaussian peaks due to SiO_4^{4-} monomer, $Si_2O_7^{6-}$ dimer and SiO_3^{2-} chain. As can be seen in this figure, most of the SiO_4 tetrahedra in the glass with the highest Li_2O content are present as the isolalted SiO_4 units such as SiO_4^{4-} monomer and $Si_2O_7^{6-}$ dimer. This fact was also recognized from our X-ray analysis and MD simulation results[4,5] of this glass. Using the Debye scattering equation[16], we calculated the reduced intensity S·i(S) curves can be seen in **Fig. 3**.

The relative intensity of each Raman band in the frequency from 800 to 1200 cm^{-1} is associated with the abundance of SiO_4 units giving rise to the stretching vibration with the Raman bands in Fig. 1. Before determining the proportions of the SiO_4 units with 1, 2, 3 and 4 NBO/Si's in the rapidly quenched Li_2O-SiO_2 glasses, we empirically checked the normalized Raman cross section of the

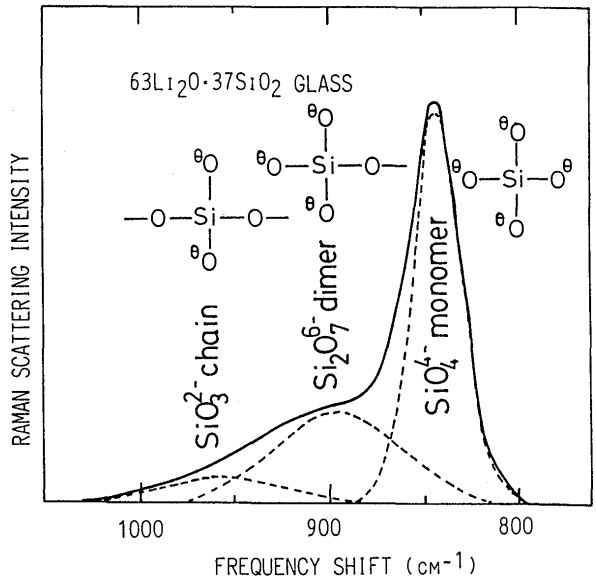

Fig. 2 Raman spectrum of $63Li_2O \cdot 37SiO_2$ glass deconvoluted into three Gaussian peaks due to SiO_3^{2-} chain, $Si_2O_7^{6-}$ dimer and SiO_4^{4-} monomer.

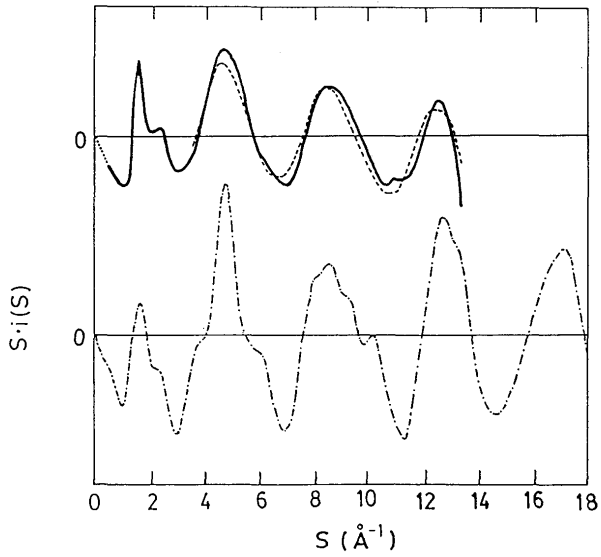

Fig. 3 Reduced intensity curves S·i(S) of $63Li_2O \cdot 37SiO_2$ glass obtained from X-ray diffraction (——), a structural model of SiO_4^{4-} monomer calculated from Debye scattering equation (·····) and Li_4SiO_4 glass derived from MD simulation[4,5] (-·-·-).

four SiO_4 units with 1, 2, 3 and 4 NBO/Si's by means of the solution of a system of linear equations, which was proposed by Mysen et al.[17,18]. The relative intensity of the Raman band i, A_i, is related to the proportion (mole fraction) of SiO_4 unit i, X_i, by the following

$$x_i = \alpha_i A_i, \qquad (5)$$

where α_i is the normalized Raman cross section of SiO_4 unit i, and A_i in the equation (5) corresponds to the area

Table 3 Relative intensity of Gaussian peaks of four SiO_4 units with 1, 2, 3 and 4 NBO/Si's, and fractions of O^0, O^- and O^{2-} in the rapidly quenched Li_2O-SiO_2 glasses.

Glass sample (mol%)	Relative intensity+ (%)				Oxygen fraction (%)		
	$Si_2O_5^{2-}$ sheet	SiO_3^{2-} chain	$Si_2O_7^{6-}$ dimer	SiO_4^{4-} monomer	O^0	O^-	O^{2-}
$63Li_2O \cdot 37SiO_2$	0	9.3	34.3	56.5	4.3	82.2	13.5
	0++	3.1++	28.1++	67.2++	5++	90++	5++
$60Li_2O \cdot 40SiO_2$	5.2	30.5	35.4	28.9	16.0	82.3	1.7
$50Li_2O \cdot 50SiO_2$	15.5	60.6	9.4	12.4	29.7	70.3	—
$41Li_2O \cdot 59SiO_2$	65.6	33.0	—	6.3	48.9	51.1	—

\+ Peak area to total area represented by equation (1).

++ MD results [4,5] of Li_4SiO_4 glass at 300K.

of the Gaussian peak i to total area represented by equation (2), that is, the relative intensity. **Table 3** lists the values of the relative intensities of these Raman bands due to the four SiO_4 units with 1, 2, 3 and 4 NBO/Si's. The α_i is then related to A_i, and is mass-balanced with the number of NBO/Si, n_i, which is 1, 2, 3 and 4 for SiO_5^{2-} sheet, SiO_3^{2-} chain, $Si_2O_7^{6-}$ dimer and Si_4^{4-} monomer, respectively. Consequently, the summation of n_i is equal to the bulk NBO/Si[17,18], which can be calculated from the analyzed composition values in Table 1 as follows

$$\sum_{i=1}^{4} \alpha_i A_i n_i = \mathrm{NBO/Si}, \qquad (6)$$

$$\sum_{i=1}^{4} \alpha_i A_i = 1, \qquad (7)$$

In the rapidly quenched Li_2O-SiO_2 glasses, the α_i factors calculated from the equations (5) ~ (7) were 1.04, 1.02, 1.15 and 0.90 for $Si_2O_5^{2-}$ sheet, SiO_3^{2-} chain, $Si_2O_7^{6-}$ dimer SiO_4^{4-} monomer, respectively. These estimated α_i factors indicate that scattering efficiency of the four SiO_4 units with 1, 2, 3 and 4 NBO/Si's is almost equivalent. Therefore, the relative intensity of the Raman bands listed in Table 3 directly corresponds to the proportions of these four SiO_4 units existing in the rapidly quenched Li_2O-SiO_2 glasses.

Figure 4 shows the proportions of the SiO_4 units with 0, 1, 2, 3 and 4 NBO/Si's and the fractions of bridging oxygen "$-O-$" or "O^0" (i. e., coordinated to two Si^{4+}), non-bridging oxygen "O^-" (i. e., coordinated to one Si^{4+}) and free or fully-active oxygen "O^{2-}" (i. e., not coordinated to Si^{4+}) in the rapidly quenched Li_2O-SiO_2 glasses as a function of the Li_2O content. The contents of $Si_2O_7^{6-}$ sheet (NBO/Si = 1) approximately have maximum at 60, 50 and 33 mole% Li_2O, respectively. These Li_2O compositions corresponds to $Li_6Si_2O_7$ (NBO/Si = 3), Li_2SiO_3 (NBO/Si = 2) and $Li_2Si_2O_5$ (NBO/Si = 1), respectively. The proportion of SiO_2^0 three-dimensional network unit (NBO/Si = 0) remarkably decrease with increasing the Li_2O content. This rapid decrease in the proportion of SiO_2^0 three-dimensional network unit with the increase of the Li_2O content is similar in trend to the considerable drop in viscosity with increassing Li_2O concentration for lithium silicate melt[21]. This result of Raman analysis illustrated in Fig. 4 suggests that any glass is not composed of only one SiO_4 unit. For example, the result that the $63Li_2O \cdot 37SiO_2$ glass consists not only of SiO_4^{4-} monomer but also of $Si_2O_7^{6-}$ dimer and SiO_3^{2-} chain suggests that the glass structure shouldarise from the following equilibrium reaction:

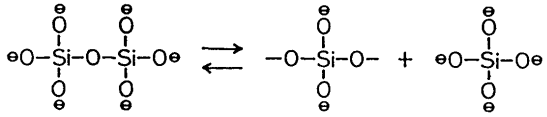

(3) (2) (4)

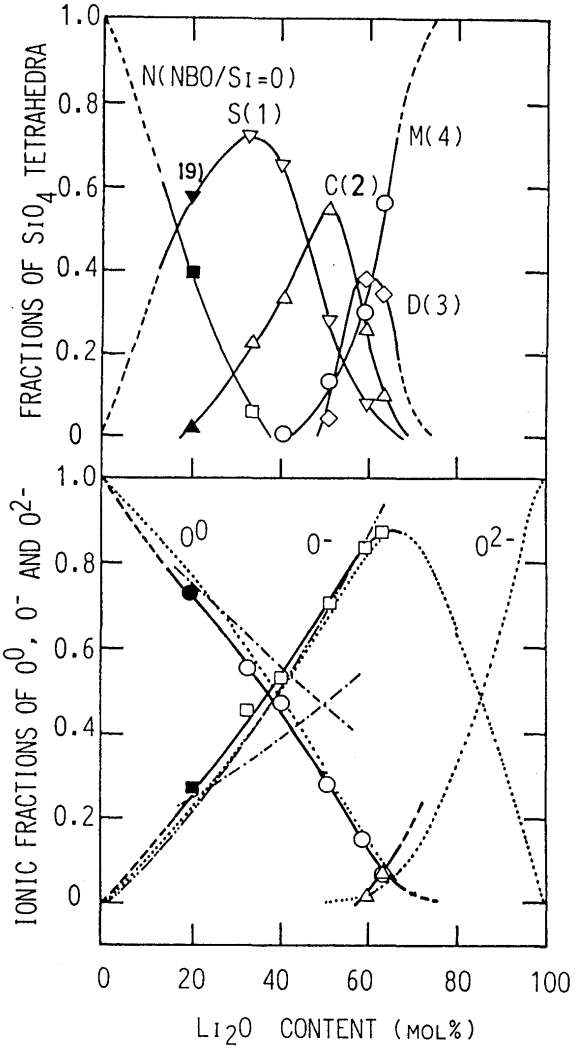

Fig. 4 Proportions of O^0, O^- and O^{2-} in the rapidly quenched Li_2O-SiO_2 glasses. Included in this figure for $Rb_2O \cdot 4SiO_2$ glass[19].
——: The proportions of O^0 and O^- obtained from XPS measurement[20].
------: The proportions of O^0, O^- and O^{2-} calculated from Yokokawa and Niwa's thermodynamical model[23] by using an optimal equilibrium constant K(=0.0078) derived from the Raman analysis.
------: The proportion of O^- can be given by $2x/(1-x)$ if the compositional formula of the rapidly quenched $Li_2O \cdot SiO_2$ glasses is regarded as $xLi_2O \cdot (1-x)SiO_2$. This curve was calculated from above mentioned equation.

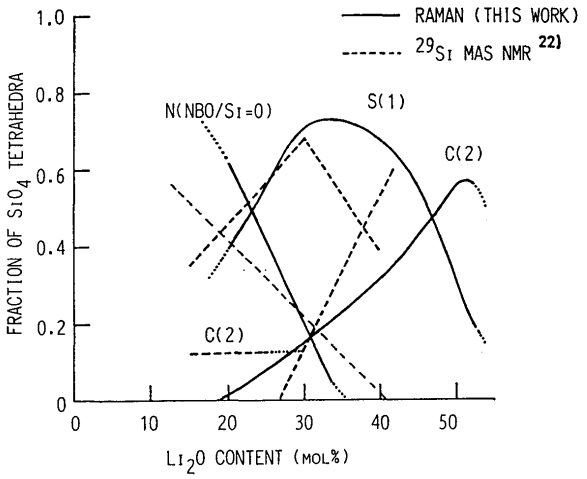

Fig. 5 Comparison of the proportions of SiO_4 units in the Li_2O-SiO_2 glasses determined by our Raman and ^{29}Si MAS NMR[22] analyses.

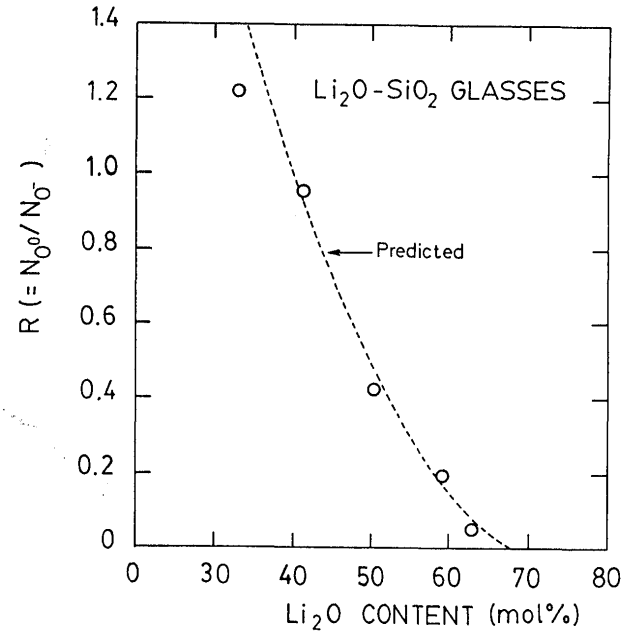

Fig. 6 Ratio of bridging to non-bridging oxygen, R ($=N_{O^0}/N_{O^-}$), in the rapidly quenched Li_2O-SiO_2 glass derived from Raman results showing agreement with the values predicted from the glass composition.

This analysis of the Raman result shows a satisfactory agreement in quantity with ^{29}Si Magic Angle Spinning NMR result[22] in the Li_2O-SiO_2 glasses ($15 \leqq Li_2O \leqq 40$ mole%) prepared by the usual melt-cooling method, as shown in **Fig. 5**. This Raman result is also in quantitatively satisfactory agreement with our MD simulation results[4,5], as indicated in Table 3.

As previously mentioned, oxygen ions in the silicate glasses can be generally classified as bridging oxygen "O^0", non-bridging oxygen "O^-" and free or fully-active oxygen "O^{2-}". As indicated in Table 3, the fractions of O^0, O^- and O^{2-} in the $63Li_2O \cdot 37SiO_2$ glass derived from the Raman result were 4%, 83% and 13%, respectively. On the other hand, the proportions of O^0, O^- and O^{2-} calculated from our MD simulations[4,5] were 5%, 90% and 5%, respectively. The agreement with these Raman and MD[4,5] values is satisfactory. Furthermore, as shown in Fig. 4(B), we compared the fractions of O^0, O^- and O^{2-} obtained from the Raman result with those calculated on the basis of a thermodynamical model proposed

by Yokokawa and Niwa[23], so that an excellent agreement in these two results can be seen. In **Fig. 6**, the ratios of bridging to non-bridging oxygen, R ($=N_{0^0}/N_{0^-}$), are compared with the values predicted for each glass from its composition and charge balance consideration. All ratios are found to agree with the predicted values. The equilibrium constant K of the following reaction between O^0, O^- and O^{2-} can be given by the following equation:

$$2O^- \rightleftharpoons O^0 + O^{2-};$$
$$K = [O^0]\cdot[O^{2-}]/[O^-]^2. \quad (8)$$

The Raman-estimated value K calculated by equation (8) is 0.0078, which is in reasonable agreement with the value of 0.14～0.003 for $M^{2+}O-SiO_2$ binary melts (M: Mn, Pb and Ca) from the thermodynamical calculation[23]. It is

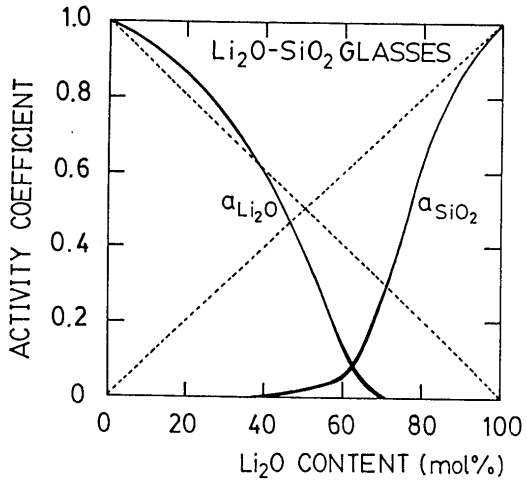

Fig. 7 Activity curves for binary Li_2O-SiO_2 glass at room temperature calculated from Yokokawa and Niwa's thermodynamical model[22] by using an optimal equilibrium constant K (= 0.0078) derived from Raman analysis.

presumed that the value K relates to the cohesive energy of network modifying oxide Ma_2O (Ma: alkali metal) such as Li_2O in the silicate melt and glass[24]. Usually a lowering of bonding strength $z_{Ma}^+/(r_{Ma}^+ : ro^{2-})$ (z_{Ma}^+: the formal charge of ion Ma^+; r_{Ma}^+ and ro^{2-}: the ionic radii of ions Ma^+ and O^{2-}) between Ma^+ and O^{2-} tends to decrease the values K[24]. It is, therefore, concluded that the value K for the $63Li_2O\cdot37SiO_2$ glass is much smaller than that for molten CaO-SiO_2 system[3]. From the obtained value K, it is possible to predict activity coefficient for silicate melts and glasses. Activity coefficient is one of the most important thermodynamical parameters. Therefore, by the use of the following Yokokawa and Niwa's equations (9) and (10) with the value K obtained, we calculated the activity curves for the Li_2O-SiO_2 glasses at room temperature, as indicated in **Fig. 7**

$$a_{SiO_2} = \left(\frac{2x_{SiO_2}}{1+x_{SiO_2}} - \frac{1-\sqrt{1-\frac{8x_{SiO_2}x_{Li_2O}}{(1+x_{SiO_2})^2}}}{2(1-4K)}\right)^2 \cdot \left(\frac{1+x_{SiO_2}}{2x_{SiO_2}}\right)^3, \quad (9)$$

$$a_{Li_2O} = \left(\frac{2x_{Li_2O}}{1+x_{SiO_2}} - \frac{1-\sqrt{1-\frac{8x_{SiO_2}x_{Li_2O}}{(1+x_{SiO_2})^2}}}{2(1-4K)}\right) \cdot \left(\frac{1+x_{SiO_2}}{2x_{Li_2O}}\right)^{3/2}, \quad (10)$$

where x_{SiO_2} and x_{Li_2O} are the mole fractions of SiO_2 and Li_2O in the glassy system Li_2O-SiO_2, respectively.

By using the proportions of the four SiO_4 units existing in the rapidly quenched Li_2O-SiO_2 glasses, we attempted to determine the average coordination numbers of the nearest-neighbor atomic pairs Si-Si, O-Si and O-O, $N_{Si/Si}$, $N_{O/Si}$ and $N_{O/O}$. We can eatimate these coordination numbers using the following two ways:

1) **Table 4** indicates the average coordination numbers of the nearest-neighbor correlations Si-Si, O-Si and O-O for the SiO_4 units with 0, 1, 2, 3 and 4 NBO/Si's, $n_{Si/Si}$, $n_{O/Si}$ and $n_{O/O}$. The relationship between the bulk's and SiO_4 unit's coordination number can be given as follows

$$N_{Si/Si} = 3f_{(NBO/Si=1)} + 2f_{(2)} + 3f_{(3)}, \quad (11)$$
$$N_{O/Si} = 1.75f_{(1)} + 1.50f_{(2)} + 1.25f_{(3)} + f_{(4)}, \quad (12)$$
$$N_{O/O} = 5.25f_{(1)} + 4.50f_{(2)} + 3.75f_{(3)} + 3f_{(4)}, \quad (13)$$

where $f_{(i)}$ ($i=1\sim4$) is the proportion of the SiO_4 unit with NBO/Si i as indicated in Table 3.

2) The fractions of O^0, O^- and O^{2-} can be given the following equations

$$N_{Si/Si} = 4N_{0^0}, \quad (14)$$
$$N_{O/Si} = 2N_{0^0} + N_{0^-}{}^{25)}, \quad (15)$$
$$N_{O/O} = 6N_{0^0} + 3N_{0^-}{}^{25)}, \quad (16)$$

where N_{0^0}, N_{0^-} and $N_{0^{2-}}$ are the fractions of O^0, O^- and O^{2-} as listed in Table 3.

The results calculated from these ways 1) and 2) are graphically in **Figures 8** and **9**, respectively. As shown in these figures, the values $N_{Si/Si}$, $N_{O/Si}$ and $N_{O/O}$ estimated from these two ways 1) and 2) reasonably drop with the increase of the Li_2O content due to the depolymerization reaction between SiO_4 units. The tendency of these coordination numbers confirms the prediction from simple consideration on the basis of compositional dependence and charge balance of alkali silicate glass structure. For instance, the $N_{O/O}$ value of the $63Li_2O\cdot37SiO$ glass is 2.7

Table 4 Coordination numbers of nearest-neighbour correlations Si-Si, O-Si and O-O for SiO_4 units with 0, 1, 2, 3 and 4 NBO/Si's.

SiO_4 unit	Bonding state of bound oxygen	NBO/Si number	Coordination number $n_{Si/Si}$	$n_{O/Si}$	$n_{O/O}$
SiO_2^0 three-dimensional network	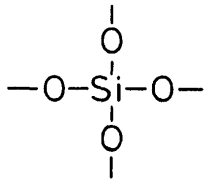	0	4.00	2.00	6.00
$Si_2O_5^{2-}$ sheet	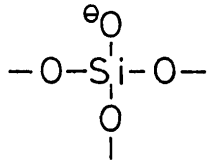	1	3.00	1.75	5.25
SiO_3^{2-} chain	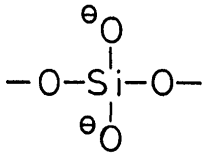	2	2.00	1.50	4.50
$Si_2O_7^{6-}$ dimer	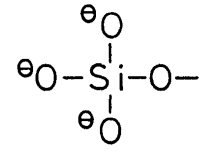	3	1.00	1.25	3.75
SiO_4^{4-} monomer	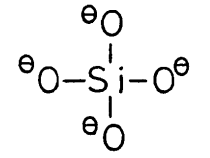	4	0	1.00	3.00

~3.4, and is almost equal to the values obtained from our X-ray diffraction result ($N_{O/O} = 3.8$) and MD simulation [4,5] ($N_{O/O} = 3.3$). Included in these two figures for comparison are the values of the coordination numbers for molten Na_2O-SiO_2 melts obtained from X-ray diffraction measurement by Waseda et al. [26] Waseda and his coworkers systematically carried out X-ray structural analyses of several alkali and alkaline earth silicate melts [27]. As shown in Figs. 8 and 9, Waseda's results indicates that the addition on Na_2O up to 60 mole% has no effect on $N_{Si/Si}$ and $N_{O/O}$ in the molten Na_2O-SiO_2 system[26], which is in no agreement with our Raman result. When Na_2O is added to SiO_2 melt and/or glass, it is well-known that the physical properties such as viscosity dramatically changes, owing to the rupture of three-dimensional network structure. Therefore, we consider that there is room for remeasurement with respect to X-ray results reported by Waseda and his coworkers[27].

The S·i(S) curves for the rapidly quenched Li_2O-SiO_2 glasses are shown in **Fig. 10**. Periodical profiles of the curves are similar to each other among these glasses with different composition. The increase of the Li_2O content, however, causes the change of the peak in the S·i(S) curves may correspond to the changing of the atomic con-

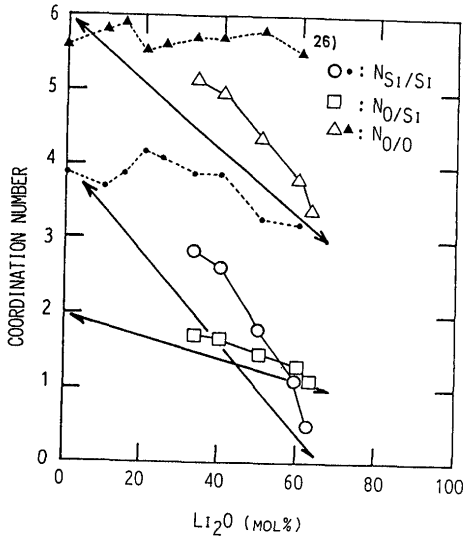

Fig. 8 Composition dependence of coordination numbers of nearest-neighbor pairs Si-Si, O-Si and O-O in the rapidly quenched Li_2O-SiO_2 glasses obtained from Raman analysis by means of way 1). The full lines represent these coordination numbers estimated from composition dependence of silicate glass structure. Included in this figure for comparison are the data for molten Na_2O-SiO_2 melts obtained from X-ray diffraction measurement by Waseda et al.[26].

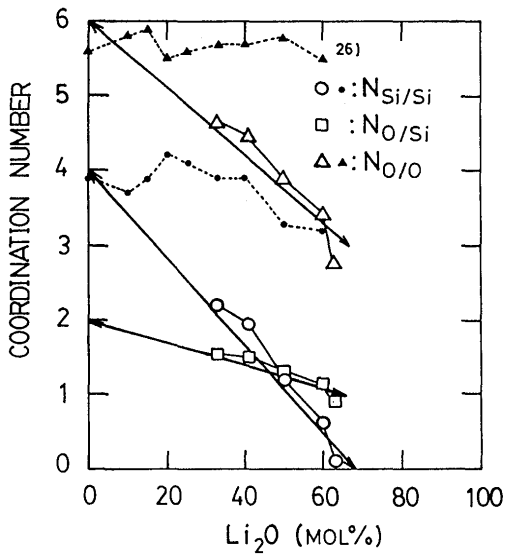

Fig. 9 Composition dependence of coordination numbers of nearest-neighbor pairs Si-Si, O-Si and O-O in the rapidly quenched Li_2O-SiO_2 glasses obtained from Raman analysis by means of way2). The full lines represent these coordination numbers estimated from composition dependence of silicate glass structure. Included in this figure for comparison are the data for molten Na_2O-SiO_2 melts obtained from X-ray diffraction measurement by Waseda et al.[26].

Table 5 Atomic distances and coordination numbers of nearest-neighbour pairs Si-O, Li-O, O-O and Si-Si in the rapidly quenched Li_2O-SiO_2 glasses determined from X-ray analysis. Include in this table for comparison are the data for lithium disilicate glasses[24, 27] and several Li_2O-SiO_2 crystals[29-32].

Glass sample (mol%)	Atomic distance (Å)				Coordination number	
	r_{Si-O}	r_{Li-O}	r_{O-O}	r_{Si-Si}	$N_{Si/O}$	$N_{Li/O}$
$63Li_2O \cdot 37SiO_2$	1.64 1.60+	2.23 1.93+	2.72 2.59+	3.20 3.10+	4.0 4.0+	3.1 3~4+
$60Li_2O \cdot 40SiO_2$	1.63	2.21	2.68	3.15	3.8	2.4
$50Li_2O \cdot 50SiO_2$	1.61	2.21	2.64	3.14	4.3	2.2
$41Li_2O \cdot 59SiO_2$	1.61	2.24	2.74	3.18	4.5	2.0
$Li_2O \cdot 2SiO_2$ (25)	1.624	—	2.65	—	3.9	—
$Li_2O \cdot 2SiO_2$ (28)	1.62	2.07	2.65	3.13	3.7	3.8
Li_4SiO_4 crystal	1.63	2.11	—	—	4	4~6
$Li_6Si_2O_7$ crystal	1.64	2.07	—	—	4	4~5
Li_2SiO_3 crystal	1.63	2.07	—	—	4	4
$Li_2Si_2O_5$ crystal	1.63	1.95	—	—	4	4

+ MD results [4,5] of Li_4SiO_4 glass at 300K.

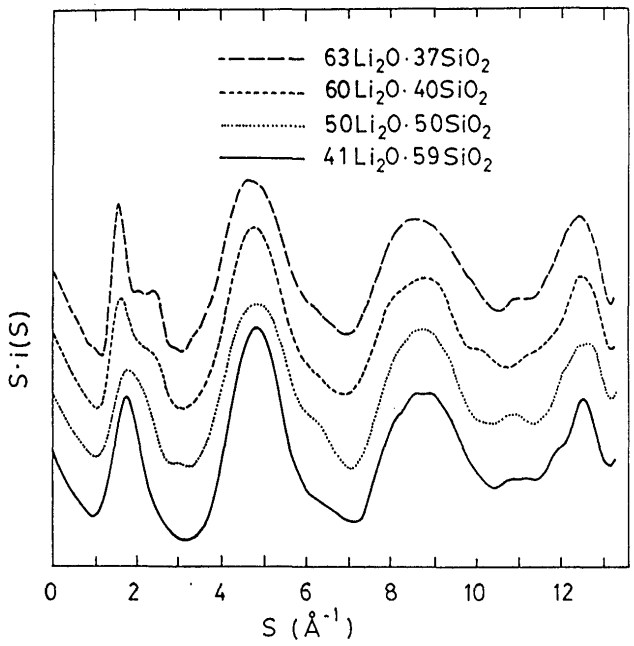

Fig. 10 X-ray reduced intensity curves S·i(S) for the rapidly quenched Li_2O-SiO_2 glasses.

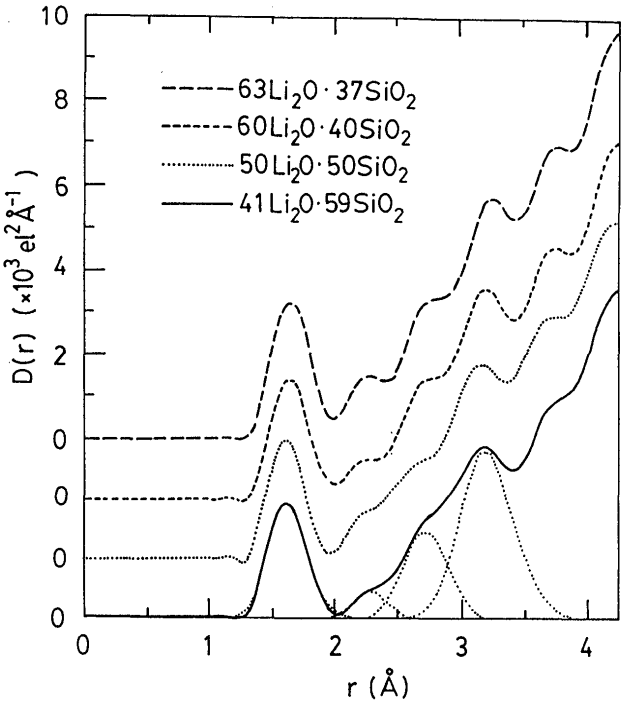

Fig. 11 Rdial distribution function curves D(r)/r for the rapidly quenched Li_2O-SiO_2 glasses.

figuration of mid- and long-range order of SiO_4 units caused by depolymerization with increasing the Li_2O content. The average atomic distances and coordination numbers for nearest-neighbor pairs Si-O, Li-O, O-O and Si-Si derived from the functions D(r)/r of **Figure 11** are listed in **Table 5**. Included in this table for comparison are the data for Li_4SiO_4, $Li_6Si_2O_7$, Li_2SiO_3 and $Li_2Si_2O_5$ crystal[29-32]. From this table, we can find the fact that the average bond length of Si-O pair, r_{Si-O}, tends to increase from 1.60 to 1.64 Å with the increase of the Li_2O content. It is considered that the elongation of Si-O bond length takes place due to the weaking of the Si-O bond produced from the introduction of modifier oxide into silicate network structure[33]. Misawa et al.[25] reported the similar elongation of the Si-O bond length in three alkali disilicate glasses from time-of-flight total neutron scattering experiment. Although the coordination numbers of nearest-neighbor oxygen around silicon, the value $N_{Si/O}$, is almost 4 because of SiO_4 tetrahedra, the coordination number around lithium, $N_{Li/O}$, is increased from 2.0 to 3.1 with increasing the Li_2O content. Compared with the lithium silicate crystals[29-32], the $N_{Li/O}$ of the glasses is much smaller than that of crystals. The small $N_{Li/O}$ is in accordance with the results of our MD simulation [4,5] for Li_4SiO_4 glass.

4. Conclusion

The result of our Raman analysis of the rapidly quenched Li_2O-SiO_2 glasses lead to the conclusion that the Raman relative intensities of the four SiO_4 units with 1, 2, 3 and 4 NBO/Si's existing in these glasses are equal to the abundance of the corresponding SiO_4 units. By the use of the proportions of the SiO_4 units and the fractions of bridging oxygen, non-bridging oxygen and free or full-active oxygen, we attempted to determine the coordination numbers of the nearest-neighbor pairs Si-Si, O-Si and O-O in the Li_2O-SiO_2 glasses. As a result, we could indicate that the obtained coordination numbers reasonably drop with the increase of the Li_2O content due to the depolymerization reaction betweeen SiO_4 units. Furthermore, in order to obtain the structural information of the Li_2O-SiO_2 glasses, X-ray diffraction measurementwas carried out. The X-ray result was found to elongate the averageatomic distance of Si-O pair with increasing the Li_2O content due to the weaking of the Si-O bonds.

References

1) M. Tatsumisago, T. Minami and M. Tanaka: J. Am. Ceram. Soc., **64** (1981), C-97.

2) M. Tatsumisago, T. Minami and M. Tanaka: J. Am. Ceram. Soc. Japan, **93** (1985), 581.

3) M. Tatsumisago, M. Tanaka and T. Minami: Chem. Express, **1** (1986), 91.

4) N. Iwamoto, N. Umesaki, M. Takahashi, M. Tatsumisago, T. Minami: J. Non-Cryst. Solids, **95/96** (1987), 233.

5) N. Umesaki, N. Iwamoto, M. Takahashi, M. Tatsumisago, T. Minami and Y. Matsui: Trans. Iron Steel Inst. Japan, **28** (1988), 852.

6) S. A. Brawer and W. B. White: J. Chem. Phys., **63** (1975), 2421.

7) B. O. Mysen, D. Virgo and C. M. Scare: Am. Mineral., **65** (1980), 690.

8) D. Virgo, B. O. Mysen and T. Kushiro: Science, **208** (1980), 1371.

9) N. Iwamoto, Y. Tsunawaki and S. Miyago: Trans. Japan Inst. Metals **43** (1979), 1138.

10) Y. Tsunawaki, N. Iwamoto, T. Hatori and A. Mitsuishi: J. Non Cryst. Solids, **44** (1981), 369.

11) T. Furukawa, K. E. Fox and W. B. White: J. Chem. Phys., **75** (1980), 3226.

12) M. Tatsumisago, M. Tanaka, T. Minami, N. Umesaki and N. Iwamoto: J. Ceram. Soc. Japan **94** (1986), 464.

13) N. Iwamoto, N. Umesaki, S. Goto, T. Hanada and N. Soga: J. Non-Cryst. Solids **70** (1985), 1775.

14) N. Iwamoto, N. Umesaki and K. Dohi: J. Japan Inst. Metals **47** (1983), 382.

15) R. J. Bell and P. Dean: Discuss. Faraday Soc., **50** (1970), 55.

16) N. Umesaki, N. Iwamoto, H. Ohno and K. Furukawa: J. Chem. Soc. Faraday Trans. I, **78** (1982), 2051.

17) B. O. Mysen, L. W. Finger, D. Virgo and F. A. Seifert: Am. Mineral., **67** (1982), 686.

18) B. O. Mysen, D. Virgo and F. A. Seifert: Am. Mineral., **70** (1985), 88.

19) N. Iwamoto, N. Umesaki and K. Dohi: J. Japan Ceram. Soc., **92** (1984), 201.

20) H. Suginohara: Bull. Japan Inst. Metals, **19** (1980), 30.

21) J. O'M. Bockris, J. D. Mackenzie and J. A. Kitchener: Trans. Faraday Soc., **51** (1955), 1734.

22) C. M. Schramm, B. H. W. S. de Jong and V. E. Parziale: J. Am. Chem. Soc., **106** (1984), 4396.

23) T. Yokokawa and K. Niwa: Trans. JIM, **10** (1969a), 3.

24) K. Nakamura: THE IWATANI "EARTH SCIENCE SERIES, Vol. 3, Materials Science of The Earth, IIed., S. Akimoto and H. Mizutani, IWATANI SHOTEN Publisher p.206 225.

25) M. Misawa, D. L. Price and K. Suzuki: J. Non-Cryst. Solids, **37** (1980), 85.

26) Y. Waseda and H. Suito: Iron Steel Inst. Japan, **17** (1977), 82.

27) Y. Waseda: Prog. Mat. Sci., **26** (1981), 81.

28) Y. Waseda and J. M. Toguri: Met. Trans., **8B** (1977), 563.

29) H. Vollenkle, A. Wittmann and H. Nowotny: Mh. Chem., **99** (1968), 1360.

30) H. Vollenkle, A. Wittmann and H. Nowotny: Mh. Chem., **100** (1969), 295.

31) F. Liebau: Acta Cryst., **14** (1961) 389.

32) H. Seemann: Acta Cryst., **9** (1956), 251.

33) S. Sakka and K. Matsusita: J. Non-Cryst. Solids, **22** (1976), 57.